



Nanocomposites made from thermoplastic linear poly(urethane-siloxane) and organoclay: Composition impact on the properties

MARIJA V. PERGAL^{1*}, SANJA OSTOJIĆ², MILOŠ STEINHART³,
IVAN S. STEFANOVIĆ¹, LATO PEZO² and MILENA ŠPÍRKOVÁ³

¹University of Belgrade, Institute of Chemistry, Technology and Metallurgy, National Institute of the Republic of Serbia, Njegoševa 12, 11000 Belgrade, Serbia, ²Institute of General and Physical Chemistry, University of Belgrade, Studentski trg 12–16, 11000 Belgrade, Serbia and ³Institute of Macromolecular Chemistry CAS (IMC), Heyrovský Sq. 2, 16206 Prague 6, Czech Republic

(Received 23 February, revised 10 April, accepted 19 April 2022)

Abstract: Thermoplastic poly(urethane-siloxane)/organoclay nanocomposites (TPU NCs) with different hard segment content (20–55 wt. %) were prepared by *in situ* polymerization in the presence of organically modified montmorillonite as a nanofiller (Cloisite 30B; 1 wt. %). Hydroxyl-terminated ethoxy-propyl-poly(dimethylsiloxane) was used as soft segment, while 4,4'-methylene-diphenyl diisocyanate and 1,4-butanediol were the hard segment components. The study of the influence of the hard segment content on the functional properties of TPU NCs was performed by Fourier transform infrared (FTIR) spectroscopy, X-ray diffractometry (XRD), atomic force microscopy (AFM), scanning electron microscopy (SEM), dynamic mechanical thermal analyses (DMTA), differential scanning calorimetry (DSC), thermogravimetric analysis (TGA), water contact angle and water absorption tests. The results revealed that TPU NCs with the increasing hard segment content exhibit higher values of degree of microphase separation, melting temperature of the hard segments, degree of crystallinity, storage modulus (except for TPU NC-55), but lower thermal stability and hydrophobicity. TPU NC films were hydrophobic and their free surface energy was in the range from 17.7 to 24.9 mJ m⁻². This work highlights how the composition of TPU NCs would affect their functional properties and provide an additional composition intended for designing advanced TPU NC materials for special biomedical applications.

Keywords: polyurethane; clay nanofiller; composition-dependent properties; degree of microphase separation; surface properties; thermal performance.

*Corresponding author. E-mail: marijav@chem.bg.ac.rs
<https://doi.org/10.2298/JSC220223036P>

INTRODUCTION

Thermoplastic polyurethanes (TPUs) are a class of block-copolymers which are segmented with short, glassy or crystalline chains segments known as hard segments (HS), acting as physical crosslink bonds and imparting stiffness and strength, and long amorphous rubber-segments known as soft segments (SS), conferring its elastic character.¹ Because the HS and SS are incompatible, the TPU exhibits two phase microdomain morphology: a HS rich phase and a SS rich phase.¹ TPU with poly(dimethylsiloxane) (PDMS) as a SS are very important for biomedical applications because of the many unique properties of PDMS, including low glass transition temperature, low surface energy, good biocompatibility, excellent thermal stability, ultraviolet resistance and high permeability to many gases.²

In recent years, TPU nanocomposites (NCs) reinforced with layered silicates, *i.e.*, clays, have earned increased interest because they show improved properties when compared to pure TPU, as a result of the high surface area and aspect ratios of the nanofillers.^{3,4} The use of a very low percentage (≤ 5 wt. %) of layered silicates in the TPU matrix has been motivated by the silicates' potential to improve properties like thermal stability, anti-flammability, mechanical properties, improved permeation barrier, shape memory behaviour, and drugs delivery property.^{4–7} It was established that for good dispersion of clay platelets into polymer matrix, clays have to be modified with some hydrophobic surfactants, since clay platelets are hydrophilic and incompatible with a relatively hydrophobic polymer matrix.⁸ Clay is usually modified by exchanging the interlayer inorganic cations with organic long-chain cations like alkylammonium ions, which enables more favourable interactions with the desired, usually hydrophobic, matrix.⁹ According to the literature,^{10–12} intercalated or exfoliated structure, partially exfoliated or mixed exfoliated-intercalated structure, could be achieved depending on the preparation method and in correlation to strength of interfacial interactions between the polymer matrix and organoclays.

Pattanayaka and Jana¹² prepared TPU-based NCs by *in situ* polymerization. It was shown that the addition of clay before the chain extension reaction led to poor dispersion of clay platelets, while when the chain extension reaction was carried out before the addition of clay, the clay platelets were well exfoliated to the scale of individual clay layers, and the best improvement in mechanical properties was observed. Jeong *et al.*¹³ and Meng *et al.*¹⁴ showed that the microphase separation and the degree of improvement to the thermal and mechanical properties mainly depend on the degree of dispersion of clay platelets within the polyurethane matrix. Nanoclays which provide a range of aforementioned improvements to the final materials seem to be a particularly promising filler for materials based on PDMS-based TPU matrix. In our previous study,¹⁰ it was found that TPU/clay NCs with 1–10 wt.% of Cloisite 30B could be efficiently

prepared by *in situ* intercalation polymerization in solution. An intercalated structure of TPU/clay NCs was found, and for TPU NCs with low nanoclay contents (1 and 3 wt. %), a high extent of organoclay dispersion in the TPU matrix was achieved. Namely, TPU NC with 1 wt. % of organoclay represents the best balance between the clay concentration and the functional properties.¹⁰

The present article is the second part of an ongoing study in which the effects of HS content (20–55 wt. %) on the microstructure and properties of TPUs were investigated. Also, the objective of this study was to prepare a series of TPU/organoclay NCs (with different HS contents and a constant organoclay content (1 wt. %)) by *in situ* polymerization. It is of essential importance to analyse the composition-property relationships of TPU/organoclay NCs and provide guiding principles for finding the optimal thermal, thermomechanical, and surface characteristics of these materials. The use of organoclay particles indicates new possibilities for modifying TPU films with potential biomedical applications. In the present study, the influence of the HS content on the functional properties was studied by the microscopic, thermal, thermomechanical and surface analysis techniques.

EXPERIMENTAL

Materials

α,ω -Dihydroxyethoxy-propyl-poly(dimethylsiloxane) (PDMS, 99%; $M_n = 1000 \text{ g mol}^{-1}$) was supplied from ABCR GmbH, Germany. 4,4'-Methylenediphenyl diisocyanate (MDI, >98%; Aldrich) was used as received. 1,4-Butanediol (BD, 99%) was supplied from Aldrich and was purified by vacuum distillation. The clay was natural montmorillonite modified with methyl-tallow-bis-2-hydroxyethyl quaternary ammonium salt, Cloisite 30B (hereafter denoted as C30B), purchased from Southern Clay Products Inc, United States. The solvents, such as *N,N*-dimethylacetamide (DMAc, from Acros Organics, Belgium, 99%) and tetrahydrofuran (THF, 98%, from Avantor Inc., United States), were distilled before use.

Preparation of TPU NCs

A series of TPU NCs was prepared by *in situ* polymerization through the prepolymer method, including two-step reaction process as previously described¹⁰ and as presented in Supplementary material to this paper.

Characterization

Fourier transform infrared (FTIR) spectra were acquired on a Nicolet 6700 FTIR spectrometer in attenuated total reflectance (ATR) mode as previously described.¹⁰ The CO and NH regions in FTIR spectra were fitted by a Gaussian deconvolution technique, resulting in the locations and areas of all of these individual peaks (Table S-I of the Supplementary material).

X-ray diffraction (XRD) was conducted with the use of the HZG/4A powder diffractometer (Seifert GmbH, Germany) in the Bragg–Bretano geometry. The region of 2θ span from 4 to 40°. The wavelength X-rays used was 0.154 nm.

Morphological studies were carried out using a JEOL JSM-6460LV scanning electron microscope (SEM) at an acceleration voltage of 30 kV. The samples were cryo-fractured in liquid nitrogen and coated with a thin layer of gold prior to the measurements.

Atomic force microscopy (AFM) characterizations were performed on an atomic force microscope (Dimension Icon, Bruker), equipped with the SSS-NCL probe, a Super Sharp SiliconTM-SPM-Sensor (NanoSensorsTM). The AFM images of the fracture surfaces of films after previous freeze-fracturing at the temperature of liquid nitrogen were measured.

Thermogravimetric analysis (TGA) was carried out on a TA Instruments TGA Q500 thermogravimetric analyzer under nitrogen flow of 60 mL min⁻¹ and from 25 to 700 °C at a rate of 5 °C min⁻¹.

Dynamic mechanical thermal properties (DMTA) were performed on an ARES G2 rheometer (TA Instruments) at a frequency of 1 Hz, strain 0.1 %, with a heating rate of 3 °C min⁻¹ and in the temperature range from -135 to 250 °C. The measurements were carried out under torsion mode, using torsion fixture (rectangle) geometry.

Differential scanning calorimetry (DSC) tests were performed on an DSC, Q1000 (TA Instruments) calorimeter with a TA Instruments RCS cooling unit and from -90 to 200 °C, at a heating and cooling rate of 10 and 5 °C min⁻¹, respectively.

Static contact angle (*WCA*) was measured by a sessile drop method at 26 °C using a contact angle analyser (Krüss GmbH, Germany DSA100). Surface energy data were calculated from the contact angle values obtained using distilled water, formamide and diiodomethane and the acid-base theory for solids according to the van Oss–Chaudhury–Good approach (Supplementary material).¹⁵

Water absorption was investigated at room temperature by sample immersion in phosphate buffered saline (PBS, pH 7.4), for 24 h (Supplementary material). The average value of three measurements for each sample was used.

RESULTS AND DISCUSSION

The present work focused on the preparation of series of TPU NCs with different HS contents (from 20 to 55 wt. %) by *in situ* polymerization using 1 wt. % of organoclay modified by quaternary alkyl ammonium ions bearing hydroxyl groups (C30B; Fig. S-1 of the Supplementary material). The chemical structures of reactants and organoclay, as well as a simplified schematic presentation of the polymerization reaction for synthesis of TPUs, and photographs of the prepared TPU NCs are presented in Fig. S-1. The effects of HS content on structural, thermal, thermomechanical and surface properties of the TPU NCs were examined.

FTIR analysis

FTIR spectra of TPU NCs containing 1 wt. % C30B with different HS contents are shown in Fig. 1, while the band assignments are given in Table S-I of the Supplementary material. The disappearance of the -NCO stretching band at 2270 cm⁻¹ confirms that all the isocyanate groups are completely consumed during the polymerization.

Namely, the NH stretching ($\nu(\text{NH})$) and carbonyl stretching ($\nu(\text{C=O})$) regions are observed at around 3330 and 1700 cm⁻¹, respectively, which are characteristic of urethane groups. In FTIR spectra, bands at 3330 cm⁻¹ were due to the hydrogen-bonded N–H stretching, while free NH stretching bands at 3440 cm⁻¹ were also detected in the TPU NCs' spectra. These results show the fraction of hydrogen-bonded urethane NH groups increased, but free urethane NH groups

decreased with the increasing HS content, indicating a higher level of hydrogen bonding in TPU NCs with higher HS content (Table S-II of the Supplementary material).

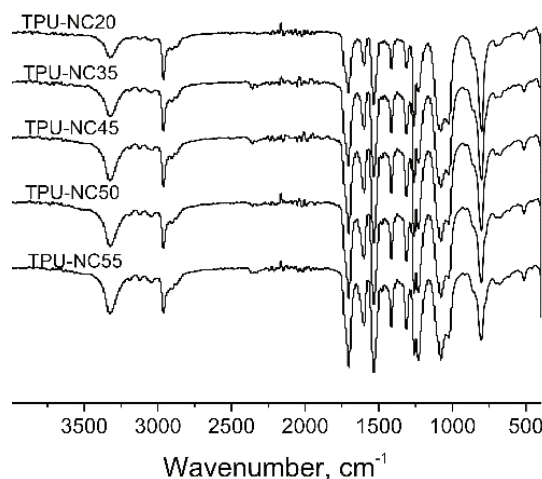


Fig. 1. FTIR spectra of TPU NCs with different hard segment content.

Carbonyl groups typically serve as proton acceptors and form hydrogen bonds with NH groups among hard segments in TPU-based NCs. Thus, the fraction of hydrogen bonded carbonyls can be used to characterize the degree of microphase separation.¹⁶ The ordered hydrogen bonded ($\nu(\text{C}=\text{O})$ HB-ordered), disordered hydrogen bonded ($\nu(\text{C}=\text{O})$ HB-disordered) and free ($\nu(\text{C}=\text{O})$ free) carbonyls in the prepared TPU NCs were observed at around 1705, 1720 and 1735 cm^{-1} , respectively.¹⁰ In series of TPU NCs, the increase of HS content led to the rise of relative intensity of the hydrogen-bonded $\text{C}=\text{O}$ absorption bands and reduction in the relative intensity of the free $\text{C}=\text{O}$ absorption bands, which further showed that increasing HS content could lead to stronger HS-HS hydrogen bonding and, thus, to a more segregated structure of TPUs. In the TPU NCs, the percentage of hydrogen bonding carbonyl groups as a fraction (more than 70 %) was higher than that of free groups, so the hydrogen bonding carbonyl groups play a major role in the final materials (Table S-II). The degree of phase separation (*DPS*) data showed that for the series of TPU NCs, increasing the content of HS enhanced the phase separation from 85.5 to 93.9 % (Table S-II, Eq. (S-3), of the Supplementary material). Comparing the FTIR spectra of TPU NCs with their pure TPU¹⁷ counterparts with the same HS content, it was found that the clay incorporation did not significantly change the relative intensities of the free or hydrogen-bonded urethane $\text{C}=\text{O}$ bands. The DPS data showed that for TPUs with 20 or 35 wt. % of HS, adding organoclay particles did not cause significant changes in the extent of phase separation. For TPUs containing from 45 to 60 wt.

% of HS, the incorporation of 1 wt. % of organoclay slightly enhanced the phase separation of the prepared TPU NCs, despite numerous reports suggesting that nanofillers can give rise to phase mixing.^{16,18}

Our FTIR results showed the fraction of urethane carbonyl groups participating in hydrogen bonding was also higher for the TPU NCs than for the pure TPU, previously published by Pergal *et al.*¹⁷ In a series of prepared TPU NC materials, organoclay evidently participates in hydrogen bonding between urethane carbonyl groups and $-\text{CH}_2\text{CH}_2\text{OH}$ groups inside the clay organomodifier,^{12,19} but to higher extent in the case of TPU NC with higher HS content.

XRD analysis

The XRD patterns of the prepared TPU NC films are shown in Fig. S-2 of the Supplementary material. Due to the poor scattering power of the samples the data are smeared by noise of a level so high that 1 % of C30B is completely hidden in it and any systematic behaviour is hard to be seen. However, the patterns could be decomposed by fitting using the program Fityk into three peaks the position of which didn't change, but information could be obtained from their integral intensities.

The 2θ of their relevant positions were 12.22, 17.6 and 21.9°, respectively, see Fig. S-2. Their corresponding integral intensities can be seen in the Table S-III. The behaviour of the middle peak indicates that it corresponds to the amorphous halo. We can estimate the ratio of amorphous component by dividing the integral intensity of this peak by the total integral intensity. As can be seen in the Fig. S-2, the ratio of the amorphous part decreases when the ratio of the hard component increases. This agrees with the state of starting components and products forming soft and hard segments. In the diffraction patterns of TPU NCs, the amorphous halo at 17.6° corresponds to the distribution of distances of neighbouring polymer chain segments.²⁰ The diffraction peak observed at $2\theta = 12^\circ$ is assigned to the internal structure of the PDMS chains. And finally, the peak at 2θ value of 21.9° corresponds to the crystalline part of the HS; the peak intensity generally increased with the rise of HS content. XRD thus confirmed the behaviour of TPU segments being considered to the hard as well as soft regions.

SEM analysis

Microstructural characterization of the prepared TPU NC materials was performed by SEM. The SEM micrographs of the cross-section of the investigated TPU NC films, at magnification 3000 \times , are given in Fig. S-3 of the Supplementary material. From Fig. S-3 it can be seen that the fracture surface of the TPU NCs become rougher when the organoclay was incorporated into the pure TPU matrix, previously published by Pergal *et al.*²¹ The prepared TPU NC with 20 wt. % HS had a smooth surface and more homogeneous surface morphologies, when compared to other prepared TPU NCs. Therefore, the TPU NCs

with the HS content of 35–55 wt. % have rougher and heterogeneous surface morphology, indicating the presence of more microphase separation in materials with higher HS content. The fractured-surface structure of TPU NCs was distributed with oval formations, in the range of 0.93–1.40 μm in size, composed of hard-enriched formations in TPU NCs, but they were slightly bigger in TPU NC with lower HS content. Homogeneous clay distribution was observed on all TPU NC sample surfaces, which suggested that the clay particles were uniformly dispersed within the TPUs' matrix and did not depend on HS content.

AFM

The surface topography and heterogeneity relief of the fractured TPU NCs with different HS content were examined by AFM. The 2D height and phase AFM images of TPU NCs' fractured surfaces, at both micrometer ($10 \times 10 \mu\text{m}^2$) and nanometer scales ($1 \times 1 \mu\text{m}^2$), are shown in Figs. 2 and S-4. The surface roughness coefficient values for $10 \times 10 \mu\text{m}^2$ images are given in Table S-IV.

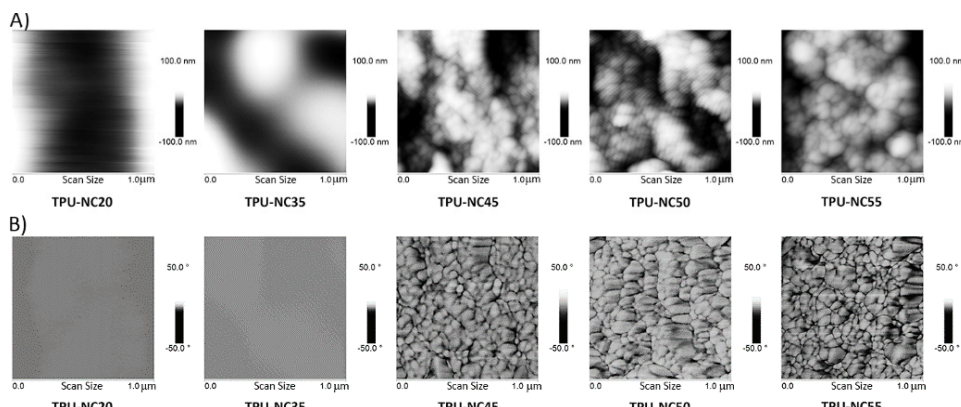


Fig. 2. A) 2D height and B) 2D phase AFM images of TPU NCs at $1 \times 1 \mu\text{m}^2$.

From Fig. S-4a it can be noted that the cryo-fractured reliefs of these TPU NCs show different surface morphologies dominated by the HS contents. Namely, the fractured surface of TPU NC with 20 wt. % of HS content is smoother and more homogenous than those of TPU-NC35, TPU-NC45, TPU-NC50 and TPU-NC55, where the formation of the two-phase morphology occurs. The AFM results are thus in accordance with the SEM analyses.

The roughness coefficients increased with increasing HS contents in TPU NC films (except TPU NC-55). Phase images shown in Fig. S-5b are in accordance with the μm -scale observations of height images given in Fig. S-5a, confirming the heterogeneous character of the prepared TPU NC films.

Deeper surface characterization of TPU NC surfaces was obtained based on the phase images and the phase images on the $1 \times 1 \mu\text{m}^2$ scale, as shown in Fig. 2.

The phase images (Fig. 2b) give information about lighter (harder) and darker (softer) areas, originating mainly from the micro-phase separation of the soft and hard segments in TPU NCs. Both “hard-enriched formations and soft-enriched formations” were observed, and these formations appeared like clusters of soft-segment and hard-segment rich regions made from smaller building units. Rougher reliefs of TPU NCs, with the HS contents higher than 45 wt. %, were detected when compared to TPU-NC20 and TPU-NC35 films.

The materials TPU-NC20 and TPU-NC35 had a relatively homogeneous phase relief with dominating softer portions (Fig. 2b), which is in accordance with the material composition. The TPU NCs with 45, 50 or 55 wt. % of HS (TPU-NC45, TPU-NC50 and TPU-NC55) were composed of individual oval or spherical harder “nanoparticles” stuck together by the softer portion into the macroscopically compact material. These oval formations were mostly about 250 to 550 nm in TPU-NC with 45–55 wt. %, and the size of the oval formations decreased with the increasing HS content.

TGA

Thermal stability of TPU-based NCs was evaluated by TGA under a nitrogen atmosphere at a heating rate of 5 °C min⁻¹. The TGA/DTG curves of TPU NCs of different compositions are presented in Fig. 3. In Table S-V of the Supplementary material, the characteristic temperatures taken from the TGA and DTG curves are summarized: the temperatures at 5, 10 and 50 wt. % loss ($t_{5\%}$, $t_{10\%}$ and $t_{50\%}$, respectively), the maximum rate degradation temperatures (t_{\max}) and the weight percent of residue. The TGA curves of TPU-based NCs indicate that the thermal degradation starts at 289–295 °C ($t_{5\%}$). The thermal stability increases with the decreasing HS content. Moreover, the thermal stability of TPU NCs was higher when compared to the pure TPU films ($t_{5\%}$, 281–286 °C),²¹ suggesting some improvement in thermal stability. Temperatures at which the pure TPU films lost 10 and 50 % of weight are ranging in 293–302 °C and in 327–335 °C, respectively.²¹ Thus, the TPU NCs were more thermally stable, which was expected in comparison to some previous findings^{5,10,22} where an improvement in thermal stability was observed with the inclusion of clay in a polymer matrix.

The improvement in thermal stability of polymer/clay nanocomposites is attributed to the shielding effect of clay layers, which function as a barrier to the gasses and volatile degradation products.²³ The clay platelets act as heat barriers and obstacles for polymer chain motion, further stabilizing the polymer chain. The effect of mineral clay, a thermal insulator and mass transport barrier, on thermal stability can be increased by improving the dispersibility of the organoclay mineral.^{8,24}

The derivative TG analysis (DTG) was used to study the thermal degradation mechanism of TPU NCs (Fig. 3b). The DTG curves indicated that the series of TPUs NCs degraded in two (from TPU-NC35 to TPU-NC55) and three (for TPU-NC20) steps; the first step (328 to 332 °C – temperature of the first peak maximum in the corresponding DTG curve) could be attributed to the degradation of the hard segments, *i.e.*, splitting of the urethane bonds, and the second step corresponded to the decomposition of PDMS segment.²⁵ The DTG curve of TPU-NC20 shows t_{\max} at 406 and 422 °C, as compared to other TPU NCs (only one t_{\max}), due to the decomposition of PDMS block and also ethylene oxide units in the SS, a consequence of the highest SS content in this sample. For the TPU NC55, t_{\max} at 506 °C is related to the decomposition of the aromatic compounds, while the second peak of degradation, corresponding to decomposition of SS, in the DTG curve for this sample did not exist due to it having the lowest SS content in the material series. In DTG curves of pure TPU films,²¹ the temperatures of the first and second peaks were observed at 313–325 °C and 338–345 °C, respectively, which are lower than that in TPU NCs films (Table S-V).

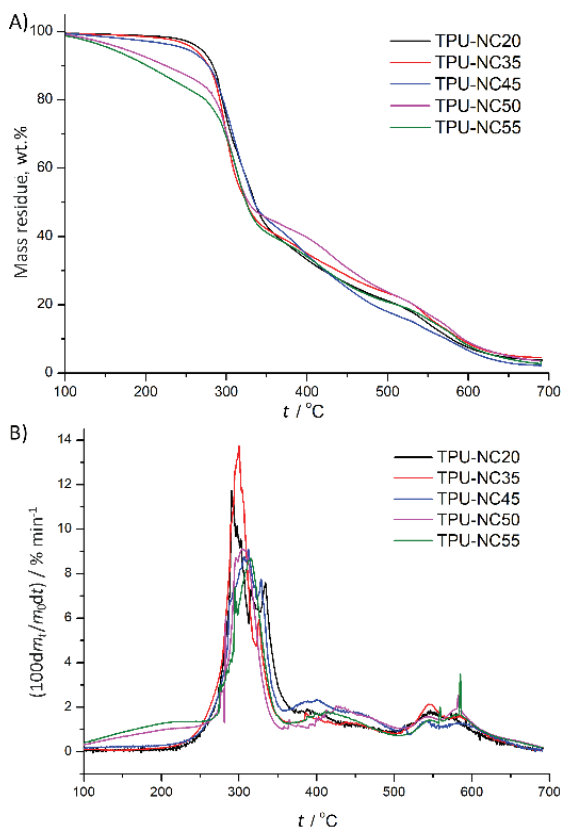


Fig. 3. A) TGA and B) DTG thermograms of TPU NCs obtained under nitrogen atmosphere.

The results indicate an enhancement of the thermal stability of the TPU NCs upon the addition of organoclays into the polymer matrix. Based on the DTG curves, it may be concluded that the addition of clay particles with the layered structure stabilizes TPU materials and, in this case, the thermal decomposition is less influenced by the HS content. Similar stabilization effects were observed in different kinds of polyurethanes reinforced with organically modified montmorillonites.^{26,27}

The residual yields of the TPU NC films at 650 °C ranged from 4.9 to 11.7 % (Table S-V) and increased with the rise of HS content. The residual yield under nitrogen originated mainly from the “organic” fraction (MDI-BD), which increased with the HS content and could be explained by the degradation mechanism of the PDMS chains under a nitrogen atmosphere that occurs after disruption of the urethane bonds. The PDMS degraded by depolymerization, giving cyclosiloxanes as the degradation products.²¹

DSC and DMTA analyses

The phase transitions in TPU NCs were examined by DMTA and DSC analyses. DMTA was performed in order to study the influence of the HS content on the viscoelastic properties of selected TPU NCs, with the HS content from 20 to 50 wt %. Two main viscoelastic parameters were analysed: the storage modulus (G') and the damping factor ($\tan \delta$). The temperature dependences of the storage modulus and the loss factor $\tan \delta$ determined by DMTA are shown in Fig. 4. Typical DMTA curves as for thermoplastic polyurethanes were found, with a t_g , rubbery plateau, melting temperature t_m , and subsequently, the flow of melted polymer.

G' and $\tan \delta$ vs. temperature curves displayed the glass transitions which were in the range from -102 to -112 °C for TPU NCs associated with the segmental motion in the PDMS SS ($t_{g\text{PDMS}}$, Table S-VI). The second relaxation observed at temperatures from -5 to 5 °C (Table S-VI) is associated with the segmental relaxation of a mixed soft phase consisting of the PDMS end group segments and some dissolved hard segments.²⁸ Therefore, this peak might be in this case related to some relaxation at the hard-soft segment interface.

From storage modulus curves, it was observed that G' increases accordingly with the HS content, which is a typical behaviour found in semi-crystalline TPUs. The storage modulus for TPU NCs increased with the HS content as a consequence of the higher degree of physical crosslinking and better microphase separation (Table S-VI). Such increase is also accompanied by the $\tan \delta$ maximum shift to higher temperatures, which took place in our case as well. In the paper published by Poręba *et al.*,⁴ on polycarbonate-based PUs with hexamethylene diisocyanate-1,4-butanediol hard segments, they observed the same trend. However, they could not detect or distinguish any peaks corresponding to the

hard segment t_g , even if the degree of crystallinity was lower than that of the HS content. In our case, it seems that this transition, also in our present study, was rather related to the hydrogen-bond disruption (t_{HBD}), or some other short-range interactions (dipol–dipol or van der Waals forces), than to the t_g of the hard MDI-BD segments (Table S-VI).⁴ Another thing is that if the polymer is in the glassy state due to hard segments below 75–125 °C, the storage modulus should be of similar value for all the samples, irrespective of the composition.⁴

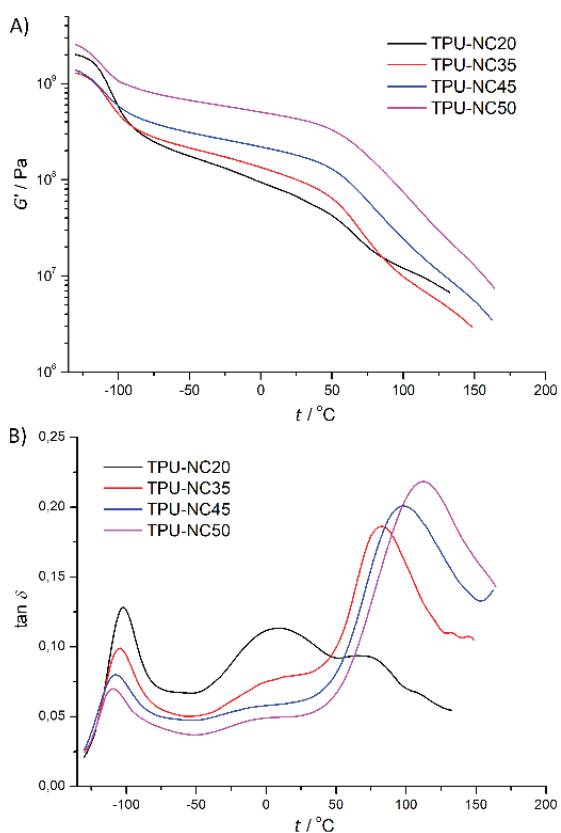


Fig. 4. A) Storage modulus and B) $\tan \delta$ of TPU NCs versus temperature.

The DSC thermograms obtained during the second heating and cooling run are shown in Fig. S-5, and the values of the interfacial relaxation (t_{rel}), the melting temperature (t_{mHS}), the enthalpy of melting (ΔH_{mHS}), the crystallization temperature (t_{cHS}), the enthalpy of crystallization (ΔH_{cHS}) and the degree of crystallinity (X_c) are presented in Table S-V. The minimum of the first endothermic event (Fig. S-5a)) (t_{rel}) assigned to the relaxation of the soft chain segments in the diffused interfacial region,⁴ was located between 60 and 112 °C for all samples, and the values for the NCs were higher by a magnitude of 28–64 °C as compared to pure TPUs.¹⁷ The relaxation enthalpy change (ΔH_{rel}) decreased

from 1.79 to 0.98 J g⁻¹ with the increasing HS content. Various endotherms in this region have been found in similar TPU-based materials and they have been attributed to different processes.⁴ A small endothermic event in this region detected on DSC curves (Fig. S-5a) was noticeable for all materials. The existence of a diffused interfacial phase between SS and HS resulted from the order-disorder relaxation of the TPU chain segments in the interface, or it suggests melting of noncrystalline HS domains in this region.⁴

The transition was in the temperature region from 153 to 206 °C detected by DSC, and it is connected with the melting temperature of HS (t_{mHS}). The multiple melting peaks which occurred in the DSC thermogram of the material with the highest HS content in our series of TPU NCs (*i.e.*, TPU-NC55) indicate the presence of crystallites of different size and perfection, due to the irregularity of the length of the hard MDI-BD segment, or to the effect of crystal reorganization during heating.²⁵

A similar trend was observed for thermal transitions determined by DSC and DMTA. It was observed that values of t_gPDMS decrease, while t_{mHS} values increase with the HS content. The obtained results showed that organoclay nanoparticles interact with hard and soft segments. The degree of crystallinity (X_c) was calculated from the values of enthalpies of melting and comparing to the heat of melting of 100 % crystalline MDI-BD homopolymer (91.2 J g⁻¹).²⁵ The degree of crystallinity of TPU NCs (from 4.6 to 9.4 %; Table S-V) is lower in comparison with series of pure TPUs.²¹ The values of X_c ranged from 4.3 to 28.5 % for the pure TPU films.²¹ The decrease in degree of crystallinity of TPU NCs could relate to the interaction of the organoclay particles with the hard segments, which makes the packing of these domains difficult.¹⁰

Water contact angle and surface free energy determination

The results of surface free energy (γ), which is important for coating applications, are presented in Table I. Surface free energy and its components were calculated using the van Oss–Chaudhury–Good approach.¹⁵ The obtained results showed that with increasing HS content, the surface free energy of TPU NCs became higher. Increasing of γ values is caused mainly by the long distance interactions between hard and soft segments γ_S^{LW} , which result from dispersion interactions of polymer chains, and also slightly from the polar interactions between functional groups of polyurethane γ_S^{AB} . The contributions from the electron-acceptor interaction slightly increased for the series of TPU NCs, while the contributions of electron-donor interaction did not change for the TPU NCs with the increasing HS content.

The water contact angles of the TPU NCs were in the range from 91.3 to 103.7°, and these values were higher than 90°, indicating the presence of hydrophobic surfaces on all prepared TPU NCs. The hydrophobicity of the TPU NC

films increased with the decreasing HS content, which is a consequence of the hydrophobic character of soft PDMS segments. Depending on the HS content, γ varied in a wide range of 17.7–24.9 mJ m⁻². The obtained results showed that the obtained TPU NCs have low values of surface free energy when compared to similar polyurethane materials presented in the literature,²⁹ suggesting good hydrophobicity characteristics of the prepared TPU NC films.

TABLE I. Static water contact angle (θ_1 / °), formamide contact angle (θ_2 / °), diiodomethane contact angle (θ_3 / °), surface free energy (γ / mJ m⁻²) and its components of the prepared TPU NCs; mean values in the same column with different superscript are statistically different at $p \leq 0.05$ level, according to post hoc Tukey's HSD test; values are given with their standard deviations

Material	θ_1	θ_2	θ_3	γ_s^{LW}	γ_s^{AB}	γ_s^+	γ_s^-	γ
TPU-NC20	103.7±5.6 ^c	92.7±3.9 ^b	84.7±2.8 ^b	15.3±0.4 ^a	2.4±0.1 ^a	1.0±0.0 ^a	1.5±0.1 ^a	17.7±0.7 ^a
TPU-NC35	100.6±3.9 ^c	90.6±5.3 ^b	81.3±3.1 ^{ab}	16.8±0.6 ^b	2.9±0.1 ^c	1.2±0.0 ^b	1.8±0.0 ^b	19.7±0.3 ^b
TPU-NC45	97.8±2.1 ^b	86.4±4.3 ^{ab}	79.5±2.6 ^b	17.7±1.0 ^{bc}	2.7±0.0 ^b	1.0±0.1 ^a	1.9±0.1 ^{bc}	20.5±0.1 ^c
TPU-NC50	96.0±3.9 ^b	84.0±5.2 ^a	77.9±2.6 ^b	18.6±1.1 ^c	2.7±0.2 ^b	1.0±0.0 ^a	2.0±0.1 ^c	21.4±0.3 ^d
TPU-NC55	91.3±2.7 ^a	81.5±2.9 ^a	72.8±3.7 ^a	21.3±0.2 ^d	3.6±0.2 ^d	1.2±0.0 ^b	2.7±0.1 ^d	24.9±0.3 ^e

Water absorption

The results listed in Table S-IV show that the weight percent of the absorbed water for TPU NCs after 24 h was between 0.5 and 1.1. These results suggest that with the HS content decrease, the water absorption becomes lower. This may be attributed to the hydrophobic character of PDMS and its surface activity.²⁹ Namely, PDMS segments can migrate to the surface of TPU NCs due to their lower surface energy in comparison to the surface energy of TPU. The obtained values of water absorption for TPU NCs were slightly lower as compared to pure TPUs, indicating higher hydrophobicity. The values of water absorption of pure TPU films ranged from 0.74 to 1.61 wt. %.²¹ The TPU NCs were more hydrophobic than the pure TPUs due to the incorporation of organoclay layers that act as barrier. The enhancement of water resistance for TPU NC films and good hydrophobicity were observed based on water absorption and contact angle measurements.

CONCLUSION

The TPU NCs were synthesized by *in situ* polymerization with different ratios of hard/soft segments and their functional properties mainly depended on their HS contents. FTIR spectroscopy analysis showed that there was a multiple hydrogen bonding in the polyurethane, but the –NH and carbonyl groups are mainly in a hydrogen bonded state. FTIR, AFM and SEM results suggested an enhanced microphase separation between soft and hard segments for TPU NCs with increasing HS content. Thermal stability increases with the decreasing HS

content, as do melting temperatures and degree of crystallinity, but the glass transition of PDMS segments decrease with the increasing HS content. Organoclay interacts with both hard and soft segments. Surface free energy values of TPU NCs increased with the rise of HS content in the range of 17.7 to 24.9 mJ m⁻². Thus, the prepared TPU NC films were hydrophobic.

The proper composition improved the selected functional properties of the TPU NCs. The improvement of thermomechanical properties were observed up to 50 wt. % of HS (except for the material with 55 wt. % of HS, which is a brittle material). From the potential practical use, the best combination of functional (thermosmechanical, thermal, water resistance and surface) properties was seen for the TPU NC films containing 50 wt. % HS. All these findings provide practical guidance for the modulation of the composition for the synthesis of advanced TPU-based composite materials. Taking into account composition, structure and properties of the TPU NCs, they can be considered as a main target as promising coatings for biomedical applications.

SUPPLEMENTARY MATERIAL

Additional data and information are available electronically at the pages of journal website: <https://www.shd-pub.org.rs/index.php/JSCS/article/view/11708>, or from the corresponding author on request.

Acknowledgments. This work was financially supported by the Ministry of Education, Science and Technological Development of the Republic of Serbia (Grant No: 451-03-68/2022-14/200026) and by the Czech Science Foundation (Grant Agency of the Czech Republic, Project No. 18-03932S). The authors are grateful to Dr Rafał Poreba (Institute of Macromolecular Chemistry CAS, Prague, Czech Republic) for DMTA measurements.

ИЗВОД

НАНОКОМПОЗИТИ НА БАЗИ ТЕРМОПЛАСТИЧНОГ ЛИНЕАРНОГ ПОЛИ(УРЕТАН-СИЛОКСАН)А И ОРГАНОГЛИНЕ: УТИЦАЈ САСТАВА НА СВОЈСТВА

МАРИЈА В. ПЕРГАЛ¹, САЊА ОСТОЈИЋ², МИЉАН СТЕИНХАРТ³, ИВАН С. СТЕФАНОВИЋ¹, ЛАТО ПЕЗО² и МИЛЕНА ЂИРКОВА³

¹Универзитет у Београду, Институт за хемију, технологију и мешавине, Институт за национално значаја за Републику Србију, Нђошева 12, 11000 Београд, ²Институт за ошину и физичку хемију, Универзитет у Београду, Студентски трг 12–16, 11000 Београд и ³Institute of Macromolecular Chemistry CAS (IMC), Heyrovsky Sq. 2, 16206 Prague 6, Czech Republic

Термопластични поли(уретан-силоксан)/органоглина нанокомпозити (TPU NCs) са различитим садржајем тврдих сегмената (20–55 теж. %) припремљени су *in situ* полимеризацијом у присуству органски модификованих монтморилонита као нанопуниоца (Cloisite 30B; 1 теж. %). Као меки сегмент коришћен је хидрокситетоксиропил терминирани поли(диметилсилоксан), а као компоненте тврдог сегмента коришћени су 4,4'-метилендифенилдиизоцијанат и 1,4-бутандиол. Проучавање утицаја садржаја тврдог сегмента на функционална својства TPU NCs је испитивано FTIR спектроскопијом, дифракцијом X-зрака (XRD), микроскопијом атомских сила (AFM), скенирајућом електронском микроскопијом (SEM), динамичко механичко термичком анализом (DMTA), диференцијално скенирајућом калориметријом (DSC), термогравиметријском анализом

(TGA), тестовима одређивања контактног угла са водом и апсорције воде. Резултати су показали да TPU NCs са већим садржајем тврдих сегмената показују веће вредности степена микрофазне сепарације, температуре топљења тврдих сегмената, степена кристаличности, модула сачуване енергије (осим за TPU NC-55), али нижу термичку стабилност и хидрофобност. TPU NC филмови су били хидрофобни и њихова површинска енергија је била у опсегу од 17,7 до 24,9 mJ m⁻². Овај рад истиче како би се променом састава у TPU NCs подешавала функционална својства и обезбедило додатно подешавање састава за дизајнирање напредних TPU NC материјала за специјалне биомедицинске примене.

(Примљено 23. фебруара, ревидирано 10. априла, прихваћено 19. априла 2022)

REFERENCES

1. Z. Petrović, J. Ferguson, *Prog. Polym. Sci.* **16** (1991) 695 ([https://doi.org/10.1016/0079-6700\(91\)90011-9](https://doi.org/10.1016/0079-6700(91)90011-9))
2. I. Yilgör, J. E. McGrath, *Adv. Polym. Sci.* **86** (1988) 1 (<https://doi.org/10.1007/BFb0025274>)
3. Y. Andriani, I. C. Morrow, E. Taran, G. A. Edwards, T. L. Schiller, A. F. Osman, D. J. Martin, *Acta Biomater.* **9** (2013) 8308 (<https://doi.org/10.1016/j.actbio.2013.05.021>)
4. R. Poręba, M. Špírková, L. Brožová, N. Lazić, J. Pavličević, A. Strachota, *J. Appl. Polym. Sci.* **127** (2013) 329 (<https://doi.org/10.1002/app.37895>)
5. M. Alexandre, P. Dubois, *Mater. Sci. Eng. Rep.* **28** (2000) 1 ([http://dx.doi.org/10.1016/S0927-796X\(00\)00012-7](http://dx.doi.org/10.1016/S0927-796X(00)00012-7))
6. S. Taheri, G. M. M. Sadeghi, *Appl. Clay Sci.* **114** (2015) 430 (<https://doi.org/10.1016/j.clay.2015.06.036>)
7. J. Pavličević, M. Špírková, O. Bera, M. Jovičić, B. Pilić, S. Baloš, J. Budinski-Simendić, *Compos., B* **45** (2013) 232 (<https://doi.org/10.1016/j.compositesb.2012.09.018>)
8. C. B. Godiya, E. Marcantoni, B. Dunjić, M. Tomić, M. S. Nikolić, J. Maletaškić, J. Djonlagić, *Polym. Bull.* **78** (2021) 2911 (<https://doi.org/10.1007/s00289-020-03248-7>)
9. Y. W. Chen-Yang, Y. K. Lee, Y. T. Chen, J. C. Wu, *Polymer* **48** (2007) 2969 (<https://doi.org/10.1016/j.polymer.2007.03.024>)
10. M. V. Pergal, I. S. Stefanović, R. Poręba, M. Steinhart, P. Jovančić, S. Ostojić, M. Špírková, *Ind. Eng. Chem. Res.* **56** (2017) 4970 (<https://doi.org/10.1021/acs.iecr.6b04913>)
11. I. S. Stefanović, M. Špírková, S. Ostojić, P. Stefanov, V. B. Pavlović, M. V. Pergal, *Appl. Clay Sci.* **149** (2017) 136 (<https://doi.org/10.1016/j.clay.2017.08.021>)
12. A. Pattanayak, S. C. Jana, *Polymer* **46** (2005) 3275 (<https://doi.org/10.1016/j.polymer.2005.02.081>)
13. E. H. Jeong, J. Yang, J. H. Hong, T. G. Kim, J. H. Kim, J. H. Youk, *Eur. Polym. J.* **43** (2007) 2286 (<https://doi.org/10.1016/j.eurpolymj.2007.03.015>)
14. X. Meng, Z. Wang, H. Yu, X. Du, S. Li, Y. Wang, Z. Jiang, Q. Wang, T. A. Tang, *Polymer* **50** (2009) 3997 (<https://doi.org/10.1016/j.polymer.2009.06.042>)
15. C. J. Van Oss, R. J. Good, M. K. Chaudhury, *Langmuir* **4** (1988) 884 (<https://doi.org/10.1021/la00082a018>)
16. J. Pavličević, M. Špírková, O. Bera, M. Jovičić, B. Pilić, S. Baloš, J. Budinski-Simendić, *Compos., B* **60** (2014) 673 (<https://doi.org/10.1016/j.compositesb.2014.01.016>)
17. M. V. Pergal, J. Nestorov, G. Toviločić, S. Ostojić, D. Godevac, D. Vasiljević-Radović, J. Djonlagić, *J. Biomed. Mater. Res., A* **102** (2014) 3951 (<https://doi.org/10.1002/jbm.a.35071>)

18. S. Shi, D. Shen, T. Xu, Y. Zhang, *Comp. Sci. Techol.* **164** (2018) 17 (<https://doi.org/10.1016/j.compscitech.2018.05.022>)
19. C.-H. Wang, Y.-T. Shieh, S. Nutt, *J. Appl. Polym. Sci.* **114** (2009) 1025 (<https://doi.org/10.1002/app.30560>)
20. M. Špírková, R. Poręba, J. Pavličević, L. Kobera, J. Baldrian, M. Pekárek, *J. Appl. Polym. Sci.* **126** (2012) 1016 (<https://doi.org/10.1002/app.36993>)
21. M. V. Pergal, I. S. Stefanović, D. Gođevac, V. V. Antić, V. Milačić, S. Ostojić, J. Rogan, J. Djonlagić, *J. Serb. Chem. Soc.* **79** (2014) 843 (<http://doi.org/10.2298/JSC130819149P>)
22. S. Sinha Ray, M. Okamoto, *Prog. Polym. Sci.* **28** (2003) 1539 (<https://doi.org/10.1016/j.progpolymsci.2003.08.002>)
23. A. Leszczyńska, J. Njuguna, K. Pielichowski, J. R. Banerjee, *Thermochim. Acta* **453** (2007) 75 (<https://doi.org/10.1016/j.tca.2006.11.002>)
24. C. M. L. Preston, G. Amarasinghe, J. L. Hopewell, R. A. Shanks, Z. Mathys, *Polym. Degrad. Stab.* **84** (2004) 533 (<https://doi.org/10.1016/j.polymdegradstab.2004.02.004>)
25. M. V. Pergal, V. V. Antić, G. Tovilović, J. Nestorov, D. Vasiljević-Radović, J. Djonlagić, *J. Biomater. Sci. Polym., E* **23** (2012) 1629 (<https://doi.org/10.1163/092050611X589338>)
26. A. K. Barick, D. K. Tripathy, *Mater. Sci. Eng., A* **527** (2010) 812 (<https://doi.org/10.1016/j.msea.2009.10.063>)
27. R. Poręba, M. Špírková, J. Pavličević, J. Budimski-Simendić, K. M. Szécsényi, B. Helló, *Compos., B* **58** (2014) 496 (<https://doi.org/10.1016/j.compositesb.2013.11.006>)
28. T. Choi, J. Weksler, A. Padsalgikar, J. Runt, *Polymer* **51** (2010) 4375 (<https://doi.org/10.1016/j.polymer.2010.07.030>)
29. P. Majumdar, D. C. Webster, *Macromolecules* **38** (2005) 5857 (<https://doi.org/10.1021/ma050967t>).